Propulsion and Power Research 2015;4(2):91–104

HOSTED BY

ELSEVIER

http://ppr.buaa.edu.cn/

Propulsion and Power Research

www.sciencedirect.com

Numerical investigation of positive dihedral application conditions in compressor cascades

Detang Zeng*, Meiyuan Li, Yongjun Zhang, Chunqing Tan

Institute of Engineering Thermophysics, Chinese Academy of Sciences, Beijing 100190, China

Received 24 September 2014; accepted 13 March 2015
Available online 29 June 2015

KEYWORDS

Dihedral;
Application conditions;
Compressor cascades;
Numerical investigation;
Aerodynamic performance

Abstract This study attempts to make a contribution to the understanding of dihedral application conditions and their aerodynamic mechanisms. The present efforts have finished contrastive investigations on several dihedral blades to their corresponding straight ones with different geometric or aerodynamic conditions including aspect ratio, solidity, aerofoil turning angle, inlet boundary layer configuration and inlet Mach number. A dihedral with the angle between the suction side and the endwall to be obtuse, i.e., positive dihedral, is chosen. The result reveals the dihedral application conditions consist of aerofoil turning angle, inlet boundary layer, inlet Mach number and so on. The further analysis indicates: in a transonic cascade, two considerations are needed on the contrastive relationship between intensities of the two shocks, namely detached shock and passage shock, and the interaction of the shocks with the corner separation.

1. Introduction

Since the idea of using dihedral-twisted blades was proposed by Filippov and Wang [1] in early 60s of the last century, dihedral blade theory research and application have undergone a satisfying development in turbine. However, up to now dihedral blade in compressor was of uncertainty. That means effects of dihedral blade are two-fold in compressor application: benefit and cost in aerodynamic performance.

Variation of flow parameter distribution along radial direction, a recognized effect of dihedral blade on flow field, causes variation of loss and performance along radial direction. Most of reported researches have focused on

*Corresponding author. Tel.: +8610 82543137.
E-mail address: zengdetang@iet.cn (Detang Zeng).

Peer review under responsibility of National Laboratory for Aeronautics and Astronautics, China.

http://dx.doi.org/10.1016/j.jppr.2015.05.005

Nomenclature

Ma	Mach number
AVDR, Φ	axial velocity density ratio
RVDR, Ψ	radial velocity density ratio
Δp	total pressure differential (unit: Pa)
h	blade height (unit: m)
C_p	static pressure coefficient
P.S	pressure surface
S.S	suction surface
HP	high pressure
3D	three dimensional
$\overline{B}$	relative chord length

Greek letters

γ	dihedral angle (unit: °)
γ_{opt}	optimal dihedral angle (unit: °)
$\overline{\overline{\omega}}$	total pressure loss coefficient
$\Delta\overline{\overline{\omega}}$	total loss improvement factor
θ	aerofoil turning angle (unit: °)
ρ	density (unit: kg/m^3); aerofoil curvature
B_s	stagger angle (unit: °)
β_T	geometric angle (unit: °)

Subscripts

MS1	inlet averagequantity
1	inlet
2	outlet
STR	straight blade
DIH	dihedral blade
m	midspan
t	tip

Superscripts

–	surface mass averaged; relative quantity
=	total mass averaged

analyzing the influences of dihedral blade on given cascades performance including secondary flow, separation, stable operation range and overall efficiency. Nevertheless, the factors which affect the effects of dihedral appear not to be fully understood and few of the correlative results are reported.

This study is aimed at searching for some dihedral application conditions, the aerodynamic or geometric factors which decide the beneficial effects of dihedral blade on overall compressor performance, and improving the understanding of the aerodynamic mechanisms of the dihedral application conditions. Based on early studies and experiences [1–16], several aerodynamic and geometric parameters are investigated consisting of inlet boundary layer (IBL), inlet Mach number, incidence, aspect ratio, solidity and aerofoil turning angle in both dihedral and straight compressors by means of CFD method. The numerical method and mesh configuration is shown in the reference [16].

1.1. Definition of dihedral

Blades are said to have dihedral when the blade surfaces are not perpendicular to either of the endwalls in pitch-wise direction [2]. Sasaki et al. [3] had also given a definition of sweep and dihedral. According to them, a lean/dihedral is introduced by moving the gravity centre of the endwall section of a blade in a direction normal to the chordline as shown in Figure 1. Lean/dihedral is 'positive' if the suction surface makes an obtuse angle with the endwall and 'negative' if it makes an acute angle with the endwall. Classified by shapes, dihedral stacking lines consist of parabola, hyperbola, double arc and multi-curved line (a line consisting of two or more curves). In this study, the multi-curved line is used to produce the positive dihedral stacking line (its detailed configuration will be told in the part Design of stacking line).

1.2. Introduction of dihedral blade in compressor

The part of compression system plays a central role in weight and cost reduction of aero-engines. In order to reduce stage count and improve performance, stage loading must rise and aerofoil boundary layers has to be well controlled as not to separate and to increase losses. The early study about custom-tailored aerofoil, as reported by Hobbs & Weingold [4], mainly focused on the aerofoil boundary layers in order to reduce the profile loss. The first approach to solve flow problems near the endwalls was end bend as given by Behlke [5] and Robinson [6]. The early concept of end bend was based on a two-dimensional way although aiming at a three-dimensional flow problem. The formation of end bend involves a given bend angle and a certain bend depth as to achieve ideal performance. In the 80s of the last century, the technology of end bend was successfully applied into the British engine of RB211-535E4 and the Chinese engine of WP7. Several years later, it was also adopted in the engine of GE-90 [7].

The introduction of dihedral blade provides another approach to change flow behavior in compressor. Actually dihedral is a further evolution of end bend technology. During the past decades, the use of dihedral in compressor has experienced more and more interest. LeJambre [8] demonstrated a 2% rise of polytropic efficiency in a multistage HP-compressor with dihedral stators. Gümme and Wenger [9] verify that dihedral stator could improve radial load contribution and control boundary layer development, furthermore reduce corner stall in hub/endwall

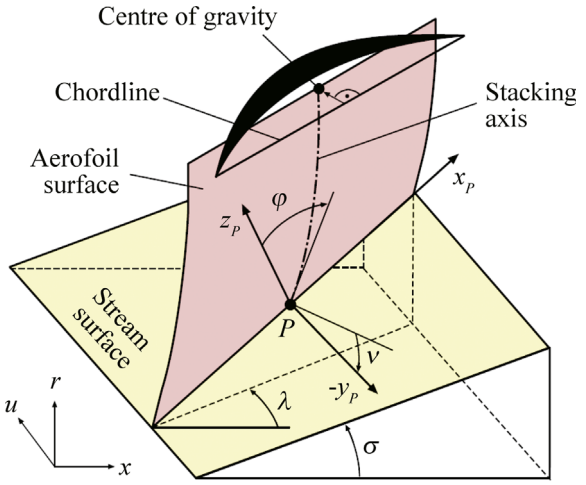

Figure 1 Definition of sweep and dihedral on a compressor aerofoil.

region by testing three-dimension flow field of dihedral blade and comparing with numerical result of the engine BR710.

Breugelmans [10] demonstrated that the prime driver for using dihedral was to add a radial blade force to the radial flow equilibrium between hub and shroud. The early discussions about the dihedral angle effect on the radial flow equilibrium by Vavra [11] and Smith [2] revealed that dihedral effect on the radial pressure gradient was proportional to the tangent of the dihedral angle. V. Gümme and U. Wenger [9] pointed out that the radial blade force changed the stream tube height and static pressure, consequently caused endwall diffusion to be alleviated. Also, they reported dihedral blade had little impact on qualitative characteristic of classical secondary flow but significantly reduced the tendency of 3D-separations and redistributed the flow structure in those blade rows dominated by 3D endwall boundary layer separations rather than classical secondary flows.

1.3. Review of previous work

Bruegelmans et al. [10] reported some dihedral effects on a rectangular compressor cascade. The blade used was NACA65 aerofoil with a chord of 100 mm, a stagger angle of 28.9° and a inlet angle of 45° corresponding to an incidence angle of −1.1° when dihedral is zero. The dihedral effect is investigated from 0° to 35° dihedral angle. The result showed a small dihedral angle (15°) produced a sufficient span-wise pressure gradient to suppress the completely-developed loss zone at the hub/endwall corner.

Lyes et al. [12] described two design/test activities which had been carried out on a 4-stage low speed research rig in Cranfield University. Most of the involved studies used a symmetrical dihedral stacking formed by a parabola. The low speed design showed an efficiency improvement of 1.5% near design point; larger improvement in efficiency was obtained near surge; stable operating range was increased significantly.

Bhaskar [13] studied dihedral effects on compressor cascades at low speed. Parabolic stacking lines were used into positive

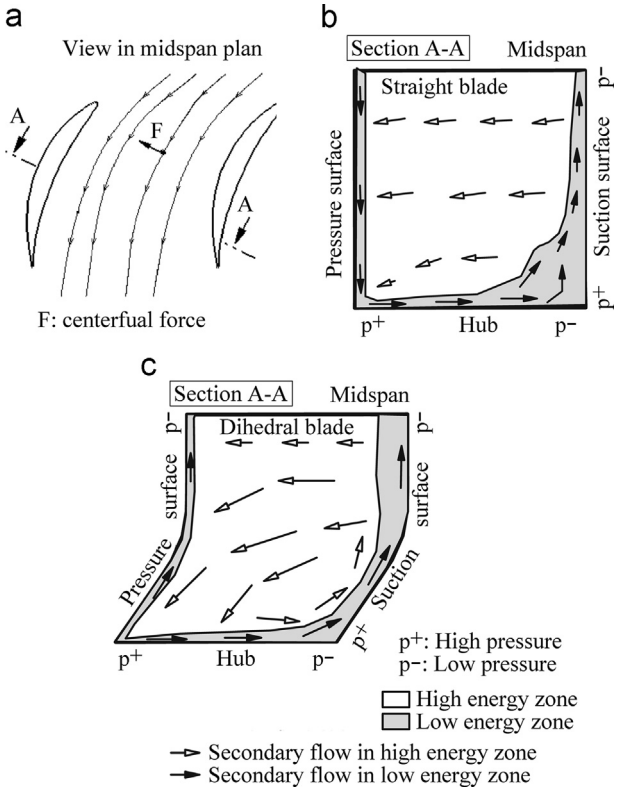

Figure 2 Effect model of dihedral blade on secondary flow. (a) A schematic of main flow, (b) secondary flow of straight cascade, and (c) secondary flow of dihedral cascade.

dihedral of 15°. Low speed cascade studies were done at 0° and 20° stagger angle. The angle of attack was varied from −10° to 20° in the 0° stagger cascade and from 0° to 35° in the 20° stagger cascade. The results showed dihedral have some beneficial and some adverse effects at the same time.

Lu [14] and Zhong [15] experimentally investigated the effects of inlet boundary layer thickness and solidity on compressors with dihedral blades respectively. The studies indicated that inlet boundary layer and solidity began to be focused as dihedral application conditions.

2. Flow mechanisms induced by dihedral

2.1. Control on separation in dihedral blade passage

A better explanation, we think, for dihedral blade to be effective in controlling the endwall flow is the rise of static pressure on the endwalls together with the decrease of low energy fluid near the endwalls, which is caused by high speed fluid immigration from middle span. A schematic model of dihedral blade in controlling secondary flow is given in Figure 2. As shown in Figure 2(a), when high speed fluid flows through cascade passage, it will be subjected to a centrifugal force pointing to the pressure side due to the turning of cascade. If the cascade is straight, the secondary flow in high speed fluid does nearly not immigrate to the endwalls (as seen in Figure 2(b)). While if

the cascade is dihedral, the composition of dihedral blade force and centrifugal force will impel some high speed fluid to immigrate to the endwalls (as seen in Figure 2(c)), which can be proved by the fact that pitched mass-averaged streamlines turn to the endwalls in the rear part of passage as seen in Figure 3. These phenomena will result in: ① The total mass of high speed fluid is increased and the flow speed is raised so as that the accumulation or separation of low energy fluid near the endwalls will be effectively controlled. ② The rise of static pressure on the endwalls strengthens the radial immigration and weakens the cross-wise immigration of low energy fluid in boundary layers, thus the accumulation or separation of low energy fluid will be further controlled.

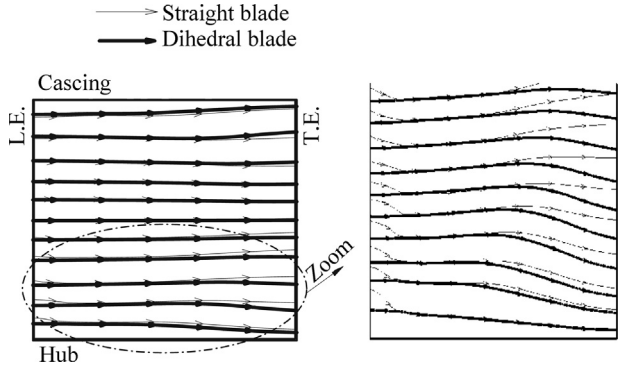

Figure 3 Pitched mass-averaged streamlines in meridian (left) and their local zoom (right).

To clarify the effect mechanism of positive dihedral blade on aerodynamic performance in compressors, a effect process about subsonic positive dihedral blade is shown in Figure 4 in which the solid lines denote positive effects and the dashed denote negative effects. Deduced from Figure 4, the factors which decide the radial immigration tendency of high speed fluid and the enhancement extent of static pressure include AVDR (axial velocity density ratio, defined as $\Phi = (V_z \times \rho)/(V_z \times \rho)_{MS1}$), aerofoil turning, dihedral angle and dihedral depth. Moreover Figure 4 also tells us that the positive blade has beneficial effects along with adverse effects at the same time. In details, the benefitsare the reductions of separation tendency and end-wall loss, while the adverse are the increases of blade friction and midspan loss. Obviously, it is appropriate to say that positive dihedral blade can improve cascade performance when the benefit effects are predominant over the adverse effects [16].

2.2. *Control on shock in dihedral blade passage*

To meet the desire of high compression ratio in compressor for advanced engine, supersonic and transonic cascades have gained rapid development. But the losses induced by shock and shock/boundary layer interaction are increased along with high compression ratio. That means the problem how to control shock intensity and lower shock loss will need to be resolved in application of dihedral blade.

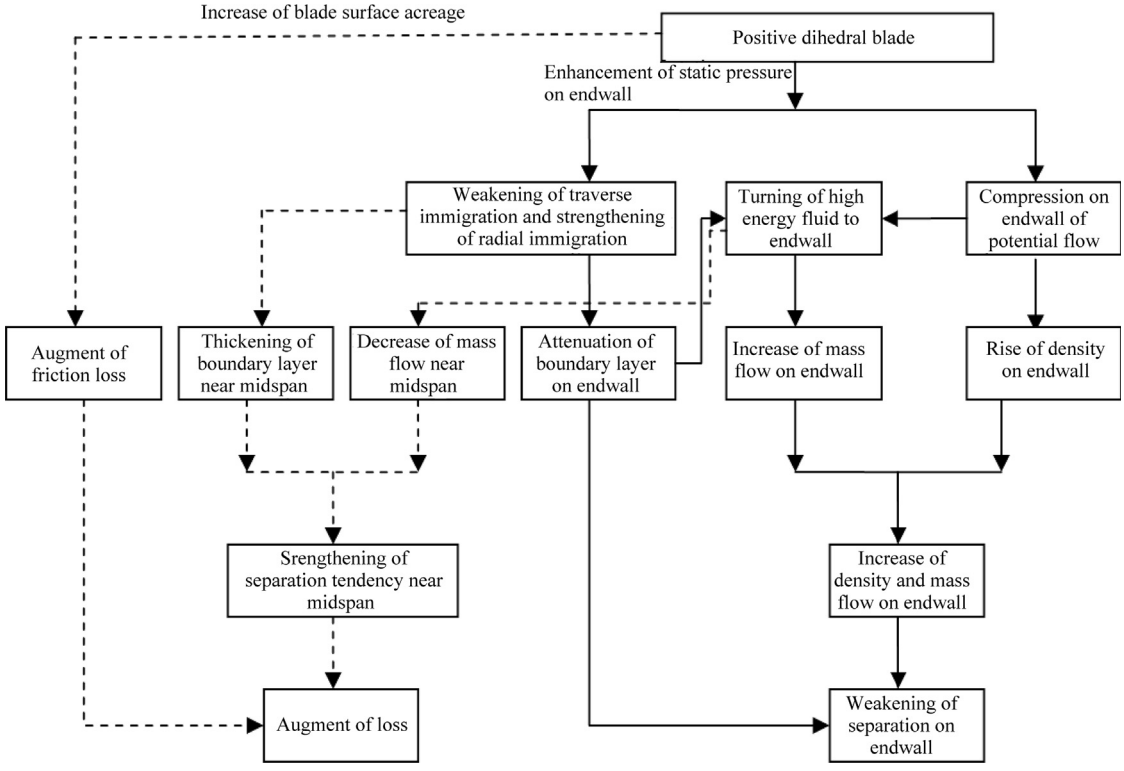

Figure 4 Mechanism process schematic of subsonic positive dihedral blade.

The distributions of aerofoil curvature for suction side and pressure side are shown in Figure 5, in which it is obvious that the curvature of detached shock-affected zone deduces gradually in the axial direction, meanwhile, the curvature of passage shock-affected zone is lower and deduces in axial direction. The aerofoil curvature directly affects the centrifugal force in cascade, and consequently affects the extent of pressure distribution changed by dihedral effect. A schematic picture of dihedral effect on pressure field of for-shock and aft-shock is shown in Figure 6(a). Three conclusions can be drawn: ① Positive dihedral blade has two effects on the detached shock. For the curvature before the detached shock is greater than after the shock, the deduction of pressure before the shock is more apparent than after the shock on midspan so as that the detached shock is strengthened ($\Delta p_{1D} > \Delta p_{1S}$). On the contrary, the rise of pressure before the shock is more apparent than after the shock near hub, thereby the shock near hub is weakened ($\Delta p_{2D} < \Delta p_{2S}$). ② Positive dihedral blade also has two effects on the passage shock. For the curvature before passage shock is greater than after the shock, the deduction of pressure before the shock is more apparent than after the shock on midspan so that the passage shock is strengthened ($\Delta p_{3D} > \Delta p_{3S}$). On the contrary, the rise of pressure before the passage shock is more apparent than after the passage shock near hub, thereby the shock near hub is weakened ($\Delta p_{4D} < \Delta p_{4S}$). ③ These dihedral effects are generally decided by intensity of shocks. The detached shock, we know, is stronger than the passage shock in high subsonic cascade, so the dihedral effects on the passage shock are somewhat weaker than on the detached shock.

As shown in Figure 6(b), both of the detached shock and the passage shock hit on the suction surface. There are four points A, B, C and D located before the detached shock, after the detached shock, before the passage shock and after the passage shock respectively. Suppose the pressure values of points B and C are equal and the pressure values of points A and D are always fixed, then the pressure relationship among the points A, B, C and D is shown in Figure 6(b)-1.When the detached shock gets stronger under dihedral effect, the pressure value of the point B (or point C) is increased due to the unchanged pressure of the point A. Furthermore the differential magnitude of pressures between the points C and D decreases due to the fixed pressure value of the point D, so the passage shock gets weaker (as shown in Figure 6(b)-2). Obviously, it is believable to say the strengthening of the detached shock will cause the weakening of the passage shock.

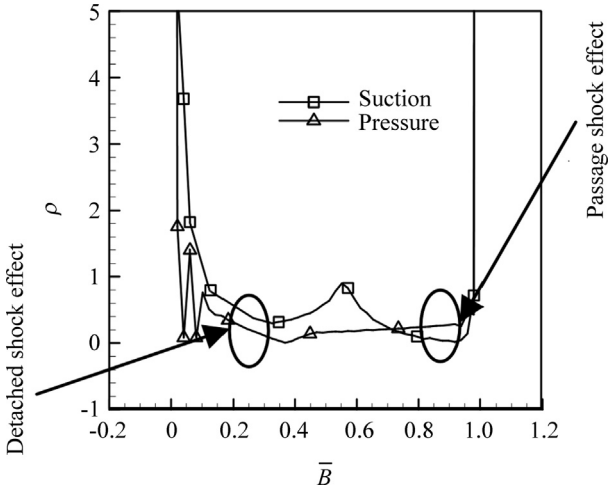

Figure 5 Blade aerofoil curvature.

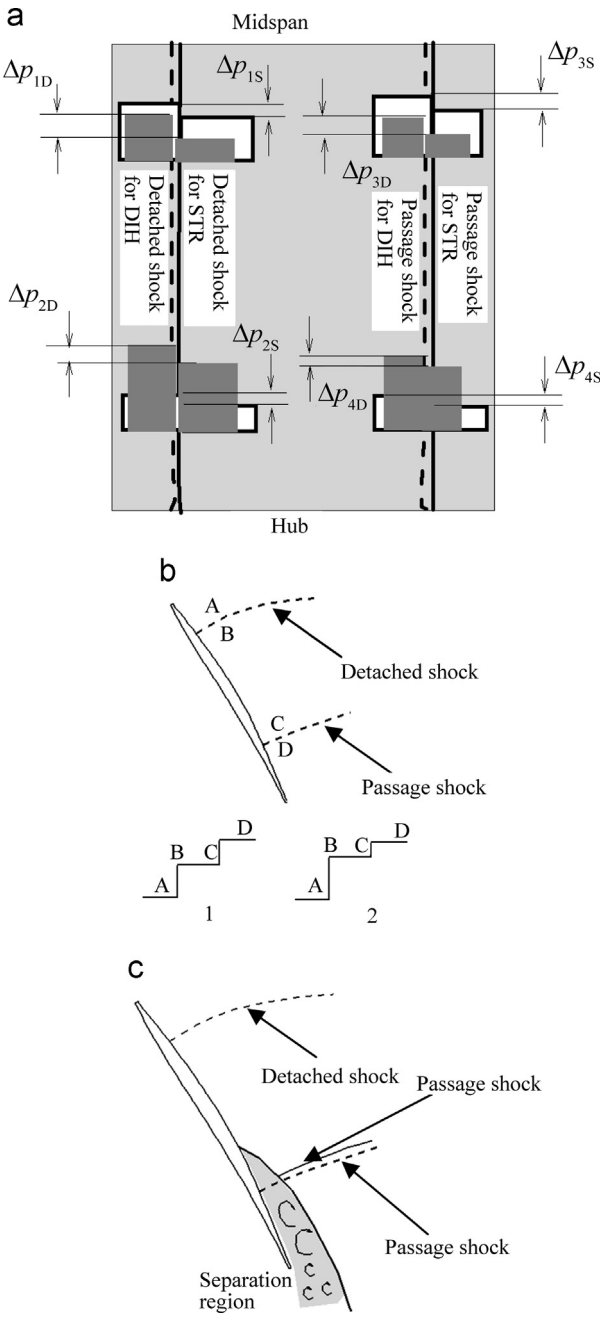

Figure 6 Schematic of positive dihedral effect on shock. (a) Effect of positive dihedral on shock pressure field, (b) interaction between shocks, and (c) effect of separation on shocks.

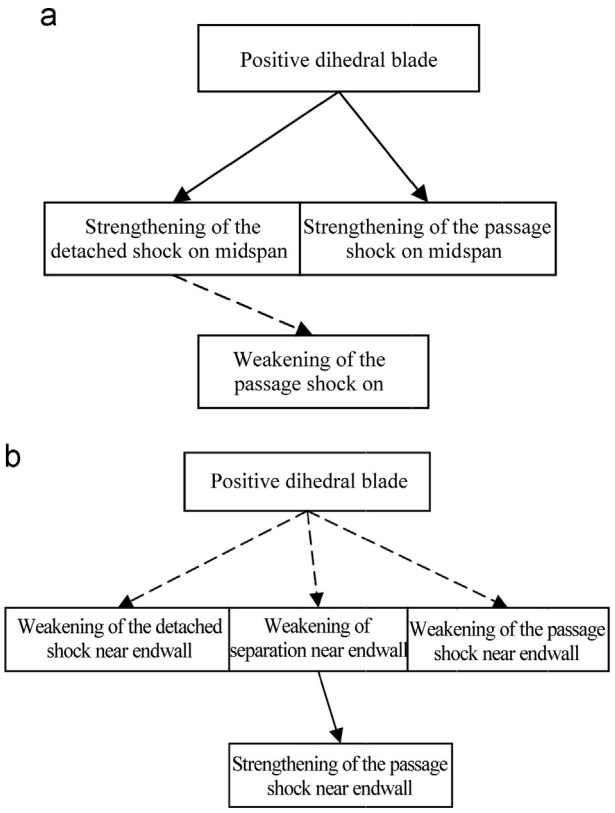

Figure 7 Mechanism process schematic of (a) supersonic and (b) transonic positive dihedral blade.

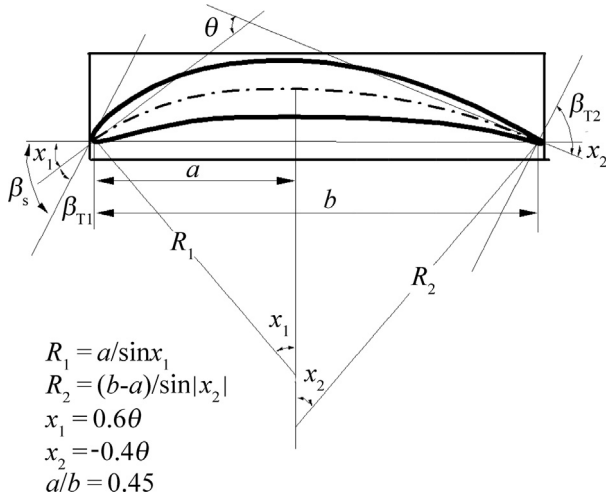

Figure 8 Design of aerofoil middle line.

In Figure 6(c), the passage shock denoted with dashed line can hit on the suction side when there is no separation on the rear part of the suction side. When there is separation, however, the passage shock denoted with solid line can not hit on the suction side through separation region and may be weakened or even distinguished for the reason that flow capacity of the cascade passage is lowered as a result of compression effect of separation region on flow passage.

So the objective of reducing shock loss and controlling flow behavior can be attained by using dihedral, which can control intensity and position of shocks through affecting pressure distributions before/after shocks and through controlling separation in supersonic and transonic cascade. To make clearer the effect mechanisms of positive dihedral blade on shocks, a process is shown in Figure 7, in which the solid lines denote positive effects and the dashed lines denote negative effects. The effects of controlling shocks

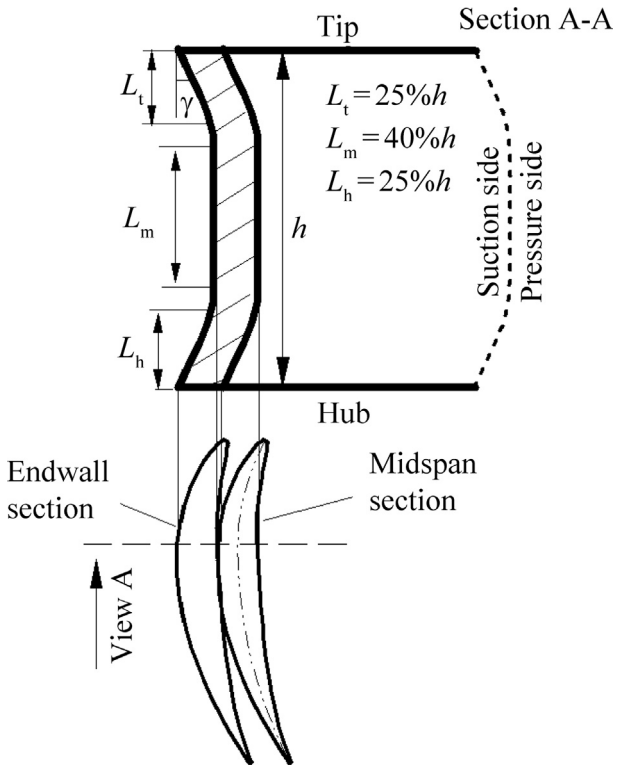

Figure 9 Dihedral stacking line.

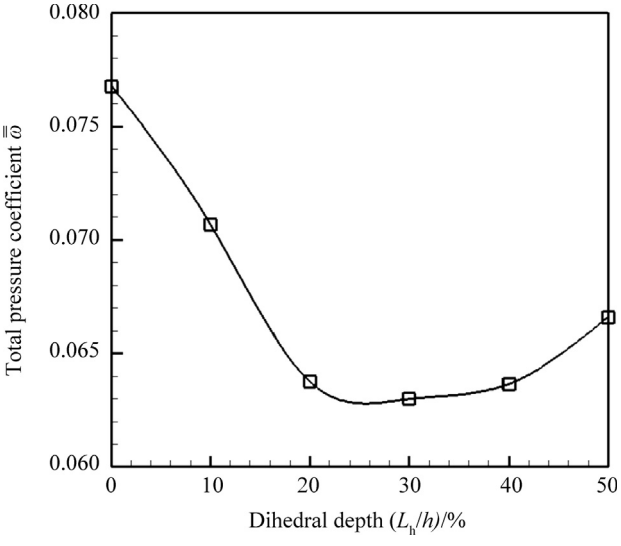

Figure 10 Variations of total pressure loss coefficient with dihedral depth.

for dihedral blade mainly rely on some factors including geometrical parameters, aerodynamic conditions and comparative relationship between intensities of the detached shock and the passage shock. Generally, positive dihedral blade has advantageous effect in lowering shock loss and improving cascade performance in high subsonic cascade, while negative dihedral blade has advantageous effect in supersonic cascade [17].

3. Computation scheme and parametric study

3.1. Design of middle arc line

The airfoils used are NACA65, CDA and TSG89-5 [18], which to be use is determined by inlet Mach number (summarized in Table 2). In Figure 8, the aerofoil middle arc lines are double-circular arcs whose equations are:

$$(x-a)^2+(y-R_1)^2=R_1^2;\quad 0\le x<a \tag{1}$$

$$(x-a)^2+(y-R_2)^2=R_2^2;\quad a\le x\le b \tag{2}$$

where $R_1=a/\sin x_1$; $R_1=(b-a)/\sin|x_2|$; $x_1=0.6\theta$; $x_2=-0.4\theta$; $a/b=0.45$. According to the equations above, if a value of turning angle θ is given, the corresponding middle arc line will be fixed; and then an aerofoil can be got through adding aerofoil thickness to the middle arc line. Finally, a analysis cascade can be obtained by using stagger angle formula $\beta_s=\beta_{T2}-x_2$, where $\beta_{T2}=-9.75^\circ$ according to the experience formula $\beta_{T2}=\delta_0+m\theta$.

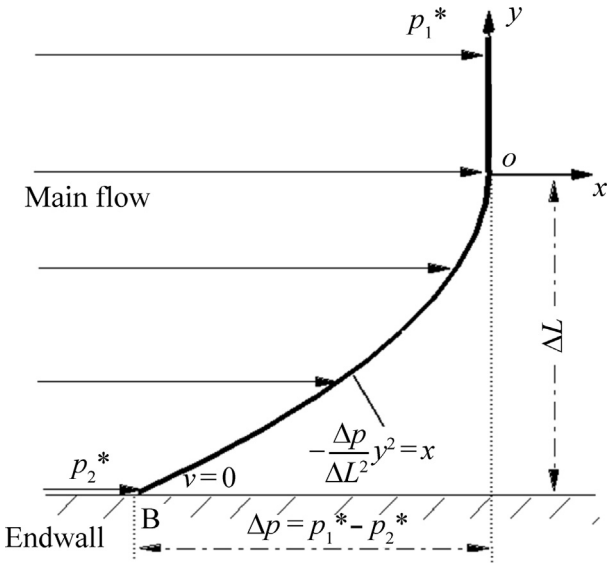

Figure 11 A schematic of inlet total pressure boundary layer.

Table 1 Cases of IBL configuration.

H_{12} ($H_{12}=\delta_1/\delta_2$)	$\Delta p/p_1^*$	$\Delta L/L$
1.09	1%	10%
1.23	2%	5%
1.25	2%	10%
1.27	2%	15%
1.48	3%	10%

3.2. Design of stacking line

It is well known that dihedral is advantageous when dihedral angle is positive, so only positive dihedral is examined here. As shown in Figure 9, the blade has a dihedral staking line symmetric about the midspan and composed of three straight lines, among which a straight central portion is connected to its neighbor dihedral portions toward the endwalls with second-order smooth curvatures. The advantageous dihedral depth is chosen as about 25% of blade height according to the loss distribution with the dihedral depths as shown in Figure 10.

3.3. Configurations of inlet boundary layer

To investigate the influence of inlet boundary layer (IBL) on dihedral, several profiles of radial total pressure distribution are given to provide different configurations of inlet boundary layer. As shown in Figure 11, the equation of total pressure profile in boundary layer is as follows [17]:

$$-\frac{\Delta p}{\Delta L^2}y^2=x \quad \text{or} \quad -\frac{p_1^*}{L^2}\bullet\frac{\Delta p/p_1^*}{(\Delta L/L)^2}y^2=x$$

Where Δp (total pressure differential) is the differential between the total pressure in main flow (p_1^*) and the total pressure near endwall (p_2^*); ΔL is boundary layer thickness; L is blade height; x is the total pressure in boundary layer at the radial position of y. Generally p_2^* is confined, namely, it has the same order as the reference pressure. In Figure 11, the derivative at the coordinate origin equals zero. Five different configurations (the form factor of boundary layer H_{12}) of IBL are set by changing $\Delta p/p_1^*$ or $\Delta L/L$ in Table 1.

Table 2 Computation cases.

Aerofoil camber angle θ	Solidity b/t
39.5°, 49.5°, 54.5°, 59.5°	1.4, 2.0, 2.6
Inlet boundary layer H_{12}	Aspect ratio h/b
0, 1.09, 1.23, 1.25, 1.27, 1.48	1.0, 1.5, 1.75
Inlet Mach number Ma	
0.25 (NACA65), 0.5, 0.7 (CDA), 0.95, 1.05 (TSG89-5)	

3.4. Computation cases

In this parametric study, whenever a parameter is changed to study its effect on dihedral, all the other parameters are fixed so as that only the effects of the parameter are determined. Here we prepare to study five geometric or aerodynamic parameters including aerofoil camber angle, solidity, aspect ratio, inlet boundary layer configuration and inlet Mach number, which are summarized in Table 2. The incidence is fixed to 0° and the dihedral angle is positive.

4. Discussions on dihedral application conditions

4.1. Overall performance

To determine the loss improvement or deterioration of dihedral blade with respect to straight blade, a variable named loss improvement factor is defined as follows:

$$\Delta\omega = \frac{(\omega_{\mathrm{STR}} - \omega_{\mathrm{DIH}})}{\overline{\overline{\omega}}_{\mathrm{STR}}}$$

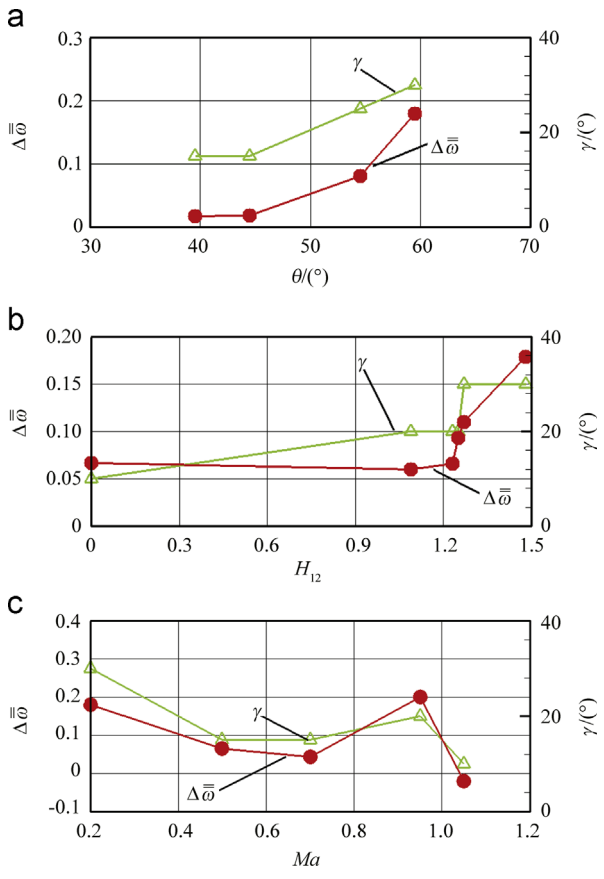

Figure 12 Optimal loss improvement factor and dihedral angle for dihedral blade with different parameters. (a) Aerofoil camber angle, (b) IBL configurations, and (c) inlet Mach numbers.

Figure 12 shows the loss improvement factor $\Delta\overline{\overline{\omega}}$ and the optimal dihedral angle γ_{opt} of dihedral blades with different geometric or aerodynamic parameters. The optimal dihedral angle is defined as a dihedral angle when a dihedral blade achieves the largest loss improvement. As seen in Figure 12(a), within the range of aerofoil camber angles studied, the blade which has the largest camber angle, i.e., 59.5° has the highest loss improvement factor, while the blade which has the smallest camber angle, i.e., 39.5° has the lowest loss improvement factor. It is obvious that the loss improvement extent of dihedral blade is gradually increased with the increase of aerofoil camber angle, so does the optimal dihedral angle with the increase of aerofoil camber angle.

With respect to the influence of IBL on the loss improvement and the optimal dihedral angle, Figure 12(b) shows loss improvement factor and optimal dihedral angle are both enhanced as a whole with the increase of the form factor H_{12} of IBL. Further efficiency improvement seems to be gained if the form factor is increased more.

In the case of inlet Mach number shown in Figure 12(c), the loss improvement and optimal dihedral angle decrease with the inlet Mach number being increased from 0.2 to 0.7, while they rise with the inlet Mach number being increased from 0.7 to 0.95 and then they decrease through sound speed limit from 0.95 to 1.05. Obviously, the loss improvement extent of dihedral is weakened by the enhancement of inlet Mach number with the absence of shock in cascade. But once shocks appear with inlet Mach number getting higher, the shock structures will add their influence to the loss improvement of dihedral as discussed in the part Control on shock in dihedral blade passage.

4.2. Aerofoil camber angle

In this section, the discussed examples about aerofoil camber angle are two cascades with aerofoil camber angles of 59.5° and 39.5°, solidity of 2.0, aspect ratio of 1.5, IBL form factor of 1.25 and inlet Mach number of 0.5. And the dihedral angle is ranged from 0° to 30° with a step of 5°. To simplify the discussion process, the abbreviations of STR595 and DIH595, STR395, DIH395 stand for straight blade with θ=59.5° and dihedral blade with θ=59.5°, straight blade with θ=39.5°, dihedral blade with θ=39.5° respectively.

Contours of axial velocity magnitude and vectors of secondary flow in the exit plane for the two camber angle cascades are compared in Figure 13. In Figure 13(a) and (b), the areas of low speed flow and back flow in the cascade DIH595 are evidently reduced and the immigration tendency of high speed flow is obviously strengthened compared with the cascade STR595. While for the cascade DIH395 as shown in Figure 13(d), the areas of low speed flow and back flow are changed a little compared with the cascade STR395 as shown in Figure 13(c).

Accordingly, the dihedral effects of different aerofoil camber angle cascades on corner separation are different. As shown in Figure 14(a), the corner-stall line, i.e. separation line on suction surface of the cascade DIH595 is much nearer to trailing edge than that of the cascade

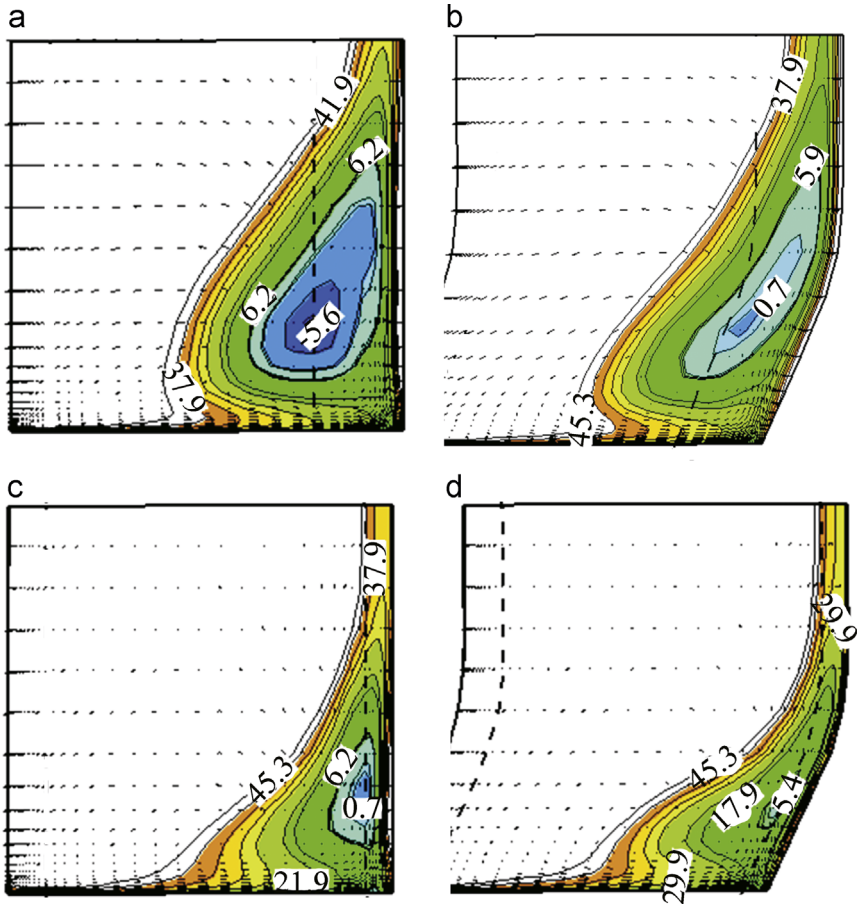

Figure 13 Contours of axial velocities and vectors of secondary exit plane. (a) STR595, (b) DIH595, (c) STR395, and (d) DIH395.

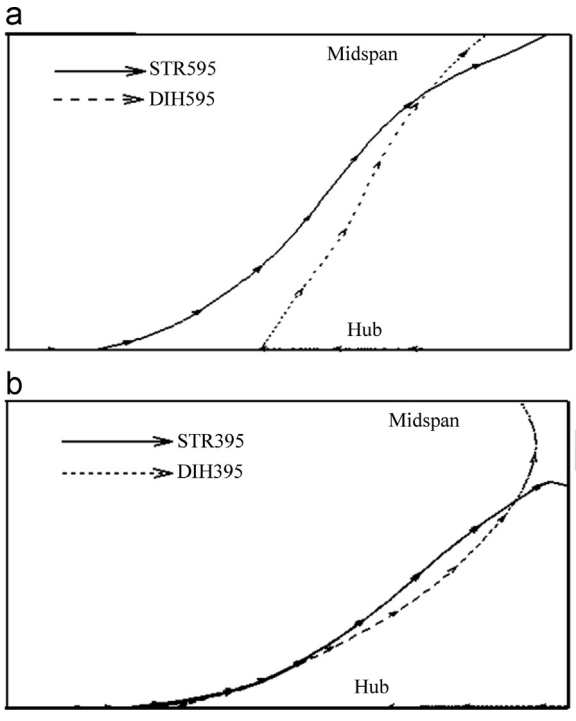

Figure 14 Corner stall lines on suction surface. (a) $\theta=59.5^\circ$ and (b) $\theta=39.5^\circ$.

STR595 and the separation region of DIH595 is much smaller than that of STR595. As seen in Figure 14(b), the variations of corner-stall line and separation region of DIH395 are negligible compared with STR395.

Contours of total pressure loss coefficients $\overline{\overline{\omega}}$ in the exit planes are shown in Figure 15. A high loss region with a loss coefficient of 0.700 in its core exists at the hub/suction corner and expands to 25% span-wise position in the cascade STR595. While in the cascade DIH595, there appear two concentrated loss regions: the one is located at the hub/suction corner; the other is located between 30% and 40% span-wise. Both of the loss cores have a loss coefficient of 0.550, which is much less than in the cascade STR595. On the contrary, the cascade DIH395 hardly improves corner loss, and the total pressure loss coefficient is kept as a value of 0.650 in the loss core as compared with STR395. Actually, higher flow turning in larger aerofoil camber angle cascade results in two facts: higher centrifugal force around the midspan and more serious separation behavior near the endwalls. Depending on these two facts, dihedral beneficial effect near the endwalls will become more dominant in larger aerofoil camber angle cascade. Loss deterioration around the midspan, however, will become more dominant than loss improvement near the endwalls in lower aerofoil camber angle cascade.

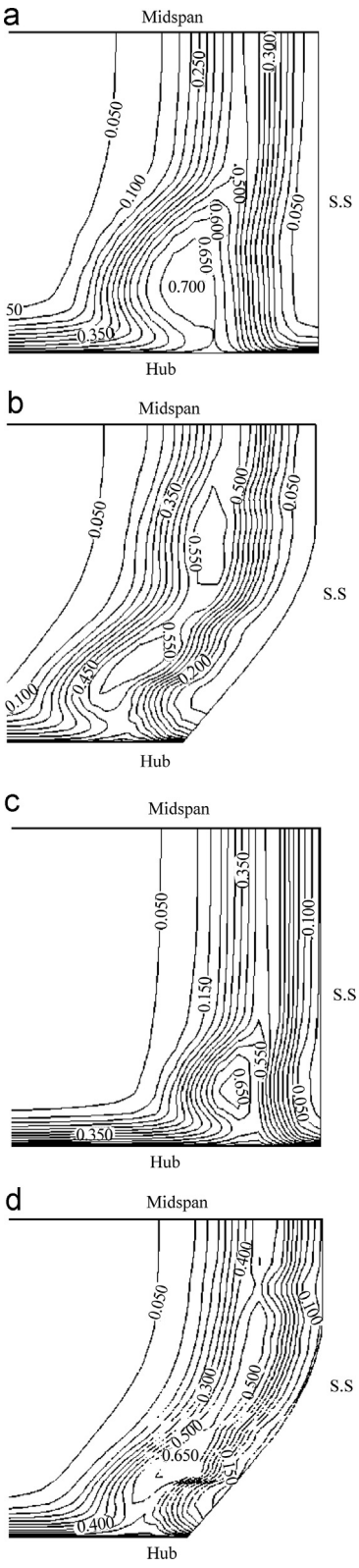

Figure 15 Contours of energy loss coefficient close to suction at exit section. (a) STR595, (b) DIH595, (c) STR395, and (d) DIH395.

4.3. Inlet boundary layer configuration

In this section, the influence of inlet boundary layer configurations on dihedral effect will be discussed. The

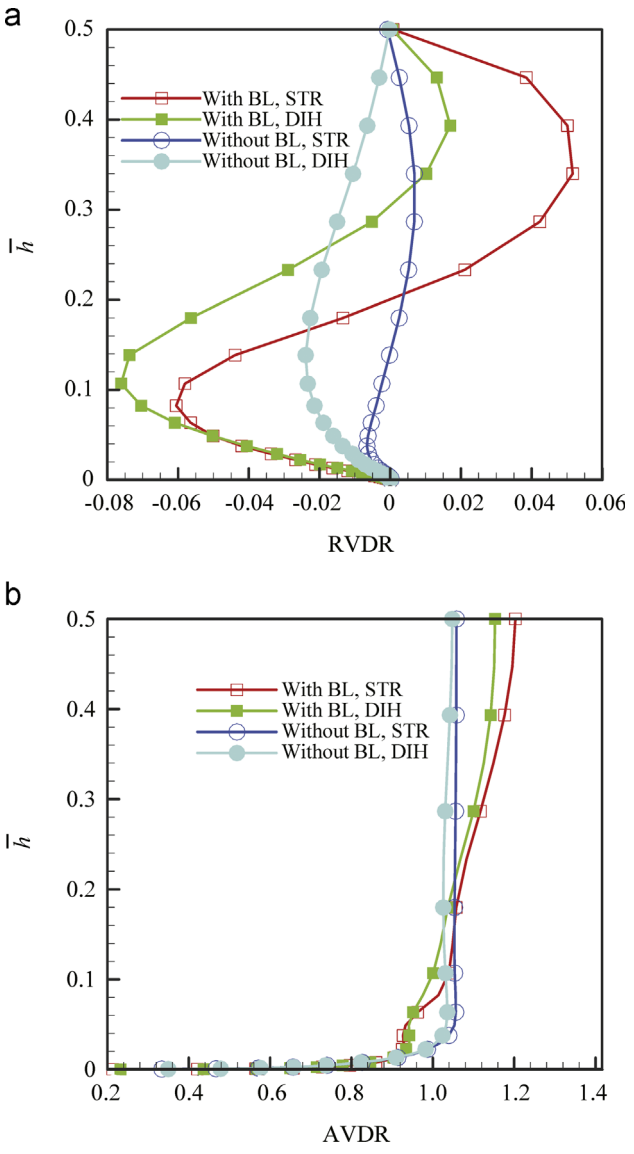

Figure 16 Mass pitch-averaged (a) RVDR and (b) AVDR distributions along span height.

cascades with H_{12} of 1.48 and 1.09 are taken as comparison examples. Figure 16(a) and (b) show mass pitch-averaged RVDR (defined as $\Psi = (V_x \times \rho)/(V_z \times \rho)_{\mathrm{MS1}}$ to imply the radial immigration tendency) and AVDR distributions along span height. In Figure 16(a), both two straight cascades show upward radial flow from about 18 per span height to the midspan and downward radial flow 18 per span height to the endwall. While comparably, dihedral cascades have stronger tendency of downward radial flow. Furthermore, downward radial flow of the dihedral cascade gets so apparent that corner stall near the endwall is easier to eliminate in the case of larger H_{12} (1.48). In Figure 16(b), the AVDR distributions show that the dihedral cascade with larger H_{12} (1.48) improves flow capacity compared to its corresponding straight cascade, which can also verify stronger ability of eliminating corner stall near the endwall

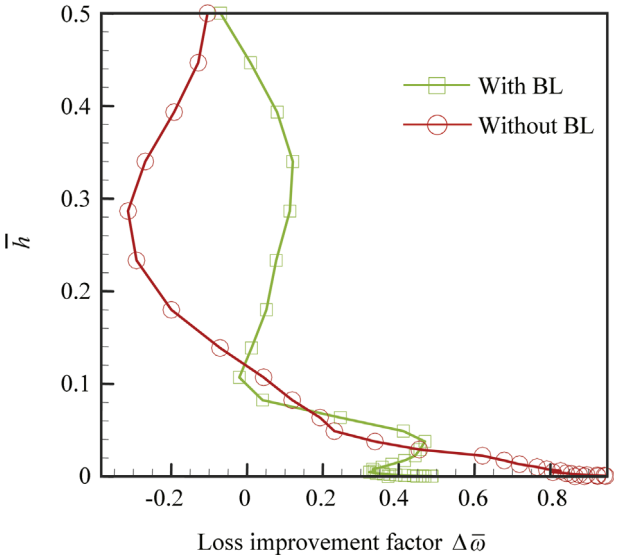

Figure 17 The loss improvement factor distributions along span height with H_{12} of 1.48 and 1.09.

for the cascade with larger H_{12} (1.48). As a result, the endwall performance of a cascade with larger H_{12} (1.48) can be apparently improved by dihedral retrofit.

In Figure 17, the loss improvement factors along span height for two types of dihedral cascade are shown. Both the curves show larger factors near the endwall and smaller factors near the midspan, which reveals that the dihedral lowers losses near the endwall and increases losses near the midspan. The dihedral blade with larger H_{12} (1.48), however, lowers more losses near the endwall than the dihedral blade with smaller H_{12} (1.09). Additionally, the dihedral blade with smaller H_{12} increases more losses near the midspan than the dihedral blade with larger H_{12}. It is obvious that dihedral will attain good effect under larger H_{12} of inlet boundary layer within the range studied.

4.4. Inlet Mach number

4.4.1. Subsonic inlet

Positive dihedral blade can, we know, effectively control separation and corner stall. That is to say that if large separation region is dominant in a cascade, dihedral blade will obtain ideal effect in improving overall performance. Thus in the condition of low inlet Mach number of 0.2, for instance, the weak flow capacity near the endwalls cause deterioration of endwall flow performance including separation and even stall, which determines dihedral blade to be very useful. But as inlet Mach number is increased, the benefit of dihedral blade in reducing losses is negligible as a result that the flow capacity near the endwalls is gradually improved and corner stall is eliminated.

Similarly, to evaluate whether a dihedral blade is efficient in improving cascade overall performance under subsonic inlet or

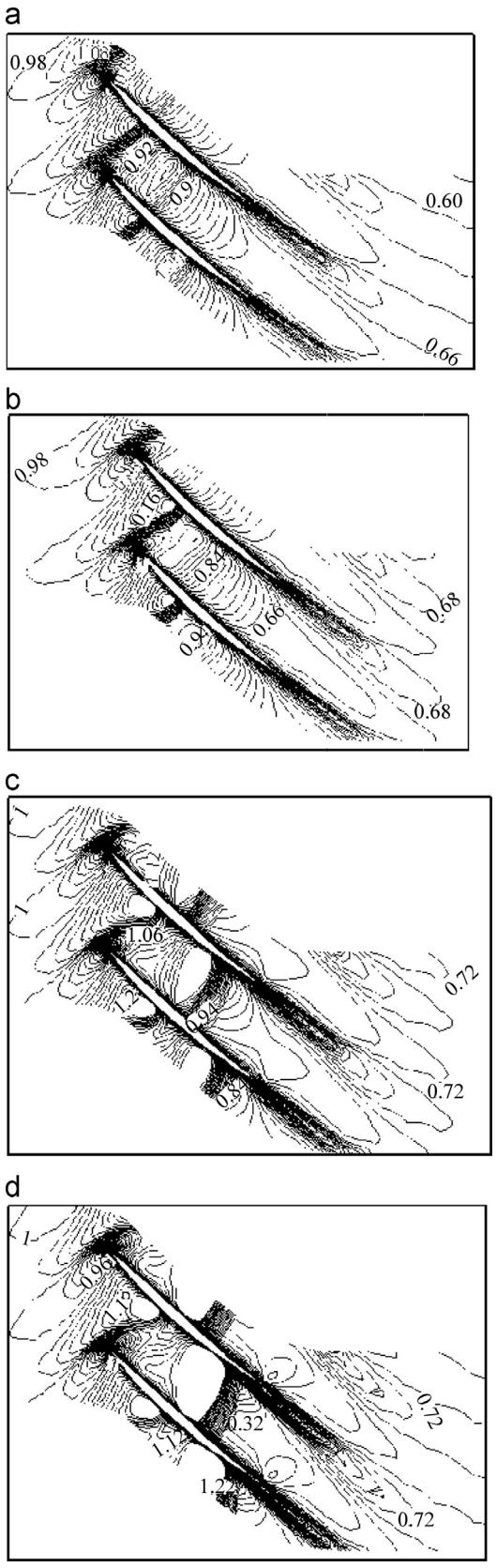

Figure 18 Contours of Mach number contour at midspan. (a) $Ma=0.95$, STR, (b) $Ma=0.95$, DIH20, (c) $Ma=1.05$, STR, and (d) $Ma=1.05$, DIH20.

not, an available way is to analyze flow behavior near the endwalls. If separation and stall are dominant near the endwalls, dihedral blade is prone to be useful. It is proved this way is well applicable in evaluating the dihedral effects under different aerodynamic or geometric parameters besides aerofoil camber angle, IBL configuration and inlet Mach number, for example, solidity and aspect ratio.

4.4.2. *Transonic inlet*

Combined with the analysis in the part control on shock of dihedral blade, further discusses about dihedral effects under transonic inlet will be focus on in this part. Figure 18 compares the contours of Mach number in the midspan sections under inlet Mach numbers of 0.95 and 1.05 between straight and dihedral blades. As shown in Figure 18(a), the detached shock is dominant and stronger than the passage shock behind it, whose rudiment has come into being but apparently weaker. After dihedral retrofit shown in Figure 18(b), the detached shock seems to get stronger, while the passage shock almost disappears. It is because the passage shock is so much weaker than the detached shock that the weakening effect of the detached shock on the passage shock is predominant over the strengthening effect of dihedral on the passage shock. Therefore, it is reasonable that the passage shock gets weaker and even disappears. In the case of inlet Mach number of 1.05 shown in Figure 18(c), however, the passage shock seems the same strong as the detached shock. Thus both the shocks get stronger after dihedral retrofit.

The static pressure distributions near the blade surfaces, i.e., blade loading, is compared at 5 per span height in Figure 19. In the case of inlet Mach number of 0.95, the pressure rise induced by the detached shock for the dihedral blade is smaller than that for the straight blade, which reveals weakening of the detached shock after dihedral retrofit. Meanwhile, dihedral blade reduces the corner separation identified by a "flattening" of the static pressure seen from the 70 per axial position to the trailing edge. In Figure 19(b), the pressure rise induced by the detached shock for the dihedral blade reveals somewhat weakening of the detached shock, also the corner separation is reduced but not as apparently as in the case of inlet Mach number of 0.95. This phenomenon will probably cause weakening of dihedral effect on the passage shock near the endwall in the supersonic cascade. Accordingly, a comprehensive schematic picture of dihedral effect on the shocks in high subsonic cascade is shown in Figure 20. It will help us understand how dihedral influences overall performance of high subsonic cascade with the present of shocks.

Figure 21 shows the distribution curves of mass pitch-averaged total pressure loss coefficient from the endwall to the midspan. According to the above-drawn conclusions, in the case of inlet Mach number of 0.95, the losses are changed little from 20 per span height to the midspan in dihedral blade compared with straight blade, while the losses are reduced a lot from 20 per span height to the

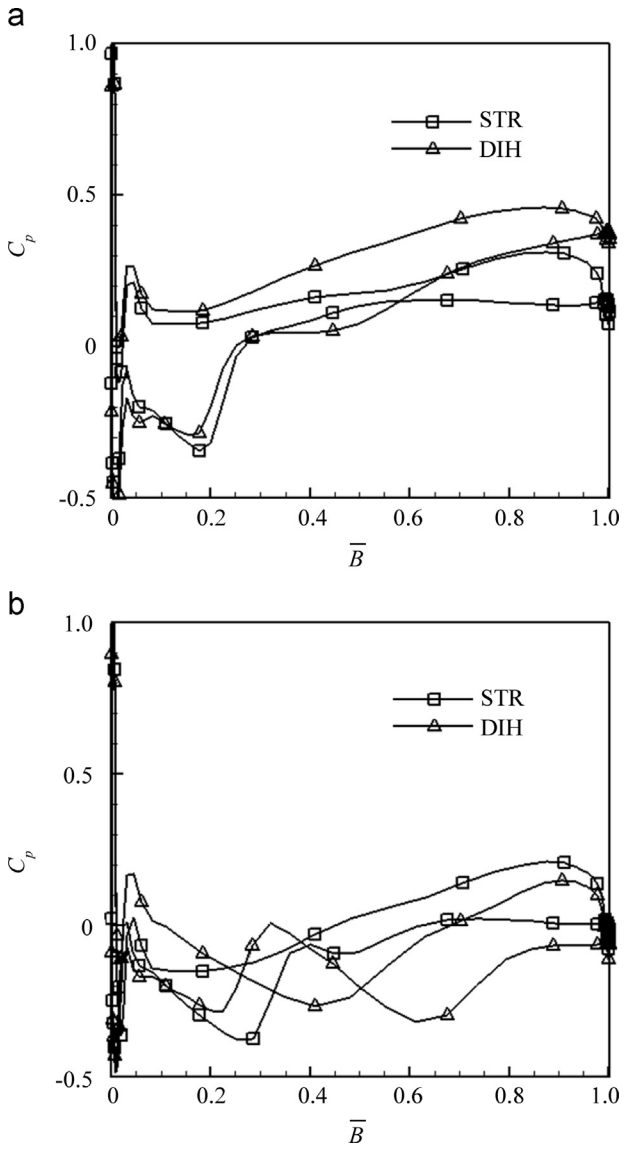

Figure 19 Surface distributions of static pressure coefficient at several blade height ($\overline{h}=5\%$). (a) $Ma=0.95$ and (b) $Ma=1.05$.

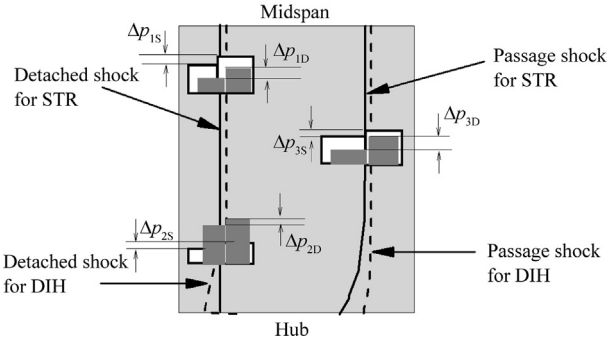

Figure 20 Effect of positive dihedral on shock along with effect on separation.

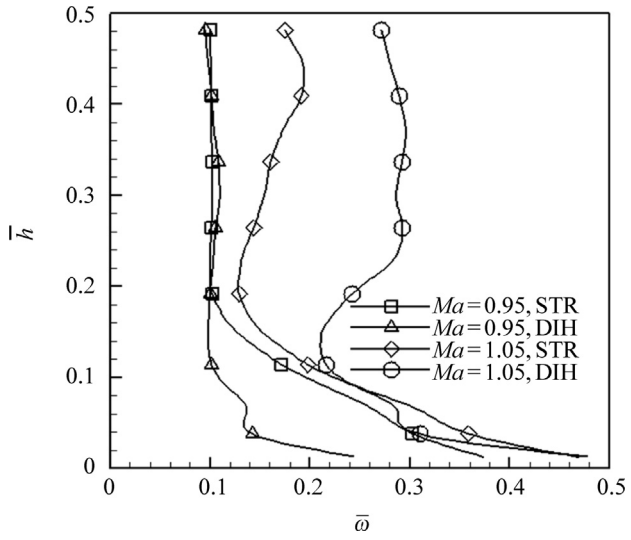

Figure 21 Distributions of mass-pitched average total pressure loss coefficient along blade height.

endwall. On the contrary, in the case of inlet Mach number of 1.05, the losses are much increased from 10 per span height in dihedral blade compared with straight blade and the losses are improved little from endwall to 10 per span height. So the overall performance is deteriorated in the case of inlet Mach number of 1.05 (as shown in Figure 12).

To sum up, how to affect cascade overall performances for positive dihedral under different inlet Mach number are partly determined by the balance between intensities of the two shocks, detached shock and passage shock, and partly determined by the interactive action of shocks with separation. In general, positive dihedral blade has advantageous effect in lowering shock loss and improving cascade performance in high subsonic cascade, while it has adverse effect in supersonic cascade as shown in Figure 12.

5. Conclusions

The authors concluded from the study:

In transonic cascades, effect mechanisms of positive dihedral are comparatively complex: firstly, positive dihedral can change intensities and positions of shocks by changing pressure differential between aft-shock and for-shock; secondly, separation change induced by dihedral will also change intensities and positions of shocks; thirdly, the change of a shock will cause the change of the other shock.

Dihedral has some beneficial and some adverse effects. The balance between the two effects is decided by some geometric or aerodynamic factors, so-called dihedral application conditions. In subsonic cascades, higher aerofoil camber angle or IBL form factor is helpful for dihedral blade to control the development of corner separation and improve aerodynamic performances. The effects of inlet Mach number on dihedral have no uniform tendency: in low subsonic cascade, higher inlet Mach number decreases the extent of improving aerodynamic performance for dihedral; in transonic cascade, higher inlet Mach number increases the extent due to the appearance of shocks; in supersonic cascade, higher inlet Mach number decreases the extent due to the change of intensity differential between the two shocks.

References

[1] M.E. Deich, A.B. Gubalev, G.A. Filippov, A new method of profiling the guide vane cascade of stage with small ratios diameter to length, Teplienergetika 8 (1962) 42–46.
[2] L.H. Smith, H. Yeh, Sweep and dihedral effects in axial - flow turbomachinery, Journal of Basic Engineering 85 (1963) 401–414.
[3] T. Sasaki, F.A.E. Breugelmans, Comparison of sweep and dihedral effects on compressor cascade performance, Journal of Turbomachinery 120 (2) (1998) 454–464.
[4] D.E. Hobbs, H.D. Weingold, Development of controlled diffusion airfoils for multistage compressor application, ASME Paper 83-GT-211, 1983.
[5] R.F. Behlke, The development of a second generation of controlled diffusion airfoils for multistage compressors, J. Turbomach 108 (1986) 32–41.
[6] C.J. Robinson, Endwall flows and blading design of axial flow compressors PhD Thesis, Cranfield Institute of Technology, Britain, 1991.
[7] Z.Y. Peng, Mechanism of Aero Gas Turbine, National Defense Publishing House, China, 2000, pp. 72–73.
[8] C.R. LeJambre, R.M. Zacharias, B.P. Biederman, A.J. Gleixner, C. Yetka, Development and application of a multi-stage Navier-Stokes flow solver - part II: application to a high pressure compressor design, ASME Paper 95-GT-343, 1995.
[9] V. Gümmer, U. Wenger, H.P. Kaur, Using sweep and dihedral to control three-dimensional flow in transonic stators of axial compressors, ASME 2000-GT-0491, 2000.
[10] F.A.H. Breugelmans, Y. Carles, M. Demuth, Influence of dihedral on secondary flow in a two dimension compressor cascade, ASME Journal of Engineering for Gas Turbine and Power 106 (3) (1984) 578–584.
[11] M.H. Vavra, Aero-thermodynamics and Flows in Turbo Machines, John Wiley and Sons, New York, 1960.
[12] P.A. Lyes, R.B. Ginder, Low-speed compressor tests of swept and bowed blade designs, ISABE 99-7048, 1999.
[13] B. Roy, P.A. Laxmiprasanna, V. Borikar, Low speed studies of sweep and dihedral effects on compressor cascades, ASME TURBO EXPO 2002, GT-2002-30441, 2002.
[14] W.C. Lu, J.J. Zhong, J.X. Su, Study on characteristic of compressor cascades with curved blades at different inlet boundary layer thickness, Journal of Harbin Institute of Technology 30 (6) (1998) 8–11.
[15] J.J. Zhong, Y.G. Liu, J.X. Su, The effects of inlet boundary layer thickness on the loss of curved blade compressor cascades, Journal of Engineering Thermophysics 18 (5) (1997) 553–557.

[16] Y.J. Zhang, F. Chen, G.T. Feng, J.X. Su, Influence of turning angles on flow field performance of linear dihedral stator in compressor at low Mach number, Chinese Journal of Aeronautics 19 (4) (2006) 271–277.

[17] Y.J. Zhang, Investigation of bowed blade controlling flow field structure and improving aerodynamic performance in diffusion cascade PhD Thesis, Harbin Institute of Technology, China, 2006.

[18] R. Fuchs, W. Steinert, H. Starken, Transonic compressor rotor cascade with boundary - layer separation: experiment and theoretical results, ASME Paper 93-GT-405, 1993.